Journal of Plant Research (2020) 133:419–428
https://doi.org/10.1007/s10265-020-01186-z

REGULAR PAPER – PHYSIOLOGY/BIOCHEMISTRY/MOLECULAR AND CELLULAR BIOLOGY

Root-knot nematodes modulate cell walls during root-knot formation in Arabidopsis roots

Takashi Ishida[1] · Reira Suzuki[2] · Satoru Nakagami[2] · Takeshi Kuroha[3,7] · Shingo Sakamoto[4] · Miyuki T. Nakata[4,8] · Ryusuke Yokoyama[3] · Seisuke Kimura[5,6] · Nobutaka Mitsuda[4] · Kazuhiko Nishitani[3] · Shinichiro Sawa[2]

Received: 24 January 2020 / Accepted: 24 March 2020 / Published online: 3 April 2020

Abstract

Phytoparasitic nematodes parasitize many species of rooting plants to take up nutrients, thus causing severe growth defects in the host plants. During infection, root-knot nematodes induce the formation of a characteristic hyperplastic structure called a root-knot or gall on the roots of host plants. Although many previous studies addressed this abnormal morphogenesis, the underlying mechanisms remain uncharacterized. To analyze the plant–microorganism interaction at the molecular level, we established an in vitro infection assay system using the nematode *Meloidogyne incognita* and the model plant *Arabidopsis thaliana*. Time-course mRNA-seq analyses indicated the increased levels of procambium-associated genes in the galls, suggesting that vascular stem cells play important roles in the gall formation. Conversely, genes involved in the formation of secondary cell walls were decreased in galls. A neutral sugar analysis indicated that the level of xylan, which is one of the major secondary cell wall components, was dramatically reduced in the galls. These observations were consistent with the hypothesis of a decrease in the number of highly differentiated cells and an increase in the density of undifferentiated cells lead to gall formation. Our findings suggest that phytoparasitic nematodes modulate the developmental mechanisms of the host to modify various aspects of plant physiological processes and establish a feeding site.

Keywords Neutral sugar analysis · Plant–microorganism interaction · Root-knot formation · Root-knot nematodes · Secondary cell wall

Introduction

Plants expand their roots into the soil. As various types of plant parasitic or symbiotic organisms live in the soil, the root appears to be the front of plant–microorganism interactions. Infection of plants with such organisms often

Takashi Ishida, Reira Suzuki and Satoru Nakagami contributed equally to this work.

Electronic supplementary material The online version of this article (https://doi.org/10.1007/s10265-020-01186-z) contains supplementary material, which is available to authorized users.

✉ Takashi Ishida
ishida-takashi@kumamoto-u.ac.jp

[1] International Research Organization for Advanced Science and Technology (IROAST), Kumamoto University, Kurokami 2-39-1, Kumamoto 860-8555, Japan

[2] Graduate School of Science and Technology, Kumamoto University, Kumamoto, Japan

[3] Graduate School of Life Sciences, Tohoku University, Sendai, Japan

[4] Bioproduction Research Institute, National Institute of Advanced Industrial Science and Technology (AIST), Tsukuba, Ibaraki, Japan

[5] Department of Industrial Life Sciences, Faculty of Life Sciences, Kyoto Sangyo University, Kyoto, Japan

[6] Center for Ecological Evolutionary Developmental Biology, Kyoto Sangyo University, Kyoto, Japan

[7] Present Address: Division of Applied Genetics, Institute of Agrobiological Sciences, National Agriculture and Food Research Organization (NARO), 2-1-2 Kannondai, Tsukuba, Ibaraki 305-8518, Japan

[8] Present Address: Division of Biological Science, Graduate School of Science and Technology, Nara Institute of Science and Technology (NAIST), 8916-5 Takayama, Ikoma, Nara 630-0192, Japan

stimulates morphological/physiological changes in plant organs. For example, nitrogen-fixing Rhizobia, clubroot-inducing Phytomyxea, and cyst-inducing cyst nematodes are microorganisms that induce abnormal organogenesis. Such irregular organ formation is observed not only in the roots, but also in the shoots; e.g., Agrobacterium induces the formation of crown galls and several species of insects produce galls on the surface of the host plant. Although these biotic-interaction-triggered organogenesis are an attractive question in the field of plant science, most cases remain descriptive and the underlying molecular mechanisms warrant elucidation.

Root-knot nematodes (RKNs) are parasitic microorganisms that infest plants. RKNs parasitize many species of rooting plants to take up nutrients, thus causing severe growth defects in the host plants. To facilitate their reproductive growth, RKNs induce the formation of characteristic swelling structures, called root-knots (RKs), on the host root by disrupting the developmental program of the plant (Bartlem et al. 2014; Jones and Goto 2011). In a single gall, several giant cells (GCs) and many surrounding neighboring cells (NCs) are induced (Cabrera et al. 2015; de Almeida Engler and Gheysen 2013; Escobar et al. 2015). Various RKN-derived effector proteins have been identified as being modulators of plant cellular mechanisms (Escobar et al. 2015).

Cell walls are a distinguishing feature of plant cells. They surround plant cells, thus determining their shape and providing mechanical strength. The primary cell wall is formed in almost all plant cells, whereas the secondary cell wall is synthesized in specifically differentiated cells, e.g., cells of vascular vessels, fiber cells, and the endothelial layer cells of anthers and seed pods (Zhong et al. 2019; Zhong and Ye 2014). The main components of the primary cell wall are cellulose, hemicellulose (xyloglucans), and pectin, while the secondary cell wall is composed of cellulose, hemicellulose (xylan and glucomannan), and lignin. Although both the primary and secondary cell wall require cellulose, plant cells express different enzymes that catalyze its synthesis. The biosynthesis of cellulose is mediated by cellulose synthase complex including heterohexamer of three different cellulose synthase subunits (CESAs) (Li et al. 2014). CESA1, CESA3, and CESA6 are required for primary cell wall formation (Arioli et al. 1998; Fagard et al. 2000; Scheible et al. 2001), whereas CESA4, CESA7, and CESA8 are necessary for the formation of the secondary cell wall in *Arabidopsis thaliana* (L.) Heynh. (Taylor et al. 1999, 2000, 2003). Therefore, timely regulation of the expression of genes related to cell wall synthesis is required for plant morphogenesis. Genes involved in the biosynthesis of cell wall components have been identified and their coordinated regulation of expression mediated by transcriptional regulations have been shown (Zhong and Ye 2014). In this context, cell wall biosynthesis should be regulated together with the cell fate; therefore, the expression of cell-wall-related genes and cell wall composition should reflect the characteristics of cells.

In this study, we analyzed time-lapse RNAseq data to elucidate the details of molecular mechanisms with a focus on the downstream consequence of gall formation by performing clustering and RT-qPCR analyses. Clustering analyses revealed that a vast number of genes were decreased in galls, including *CESA4*, *CESA7*, and *CESA8*, which suggests that the activity of secondary cell wall biosynthesis is weakened in galls. Genes that were co-expressed with *CESA4*, *CESA7*, and *CESA8* were also decreased in galls. Our RT-qPCR analyses confirmed the downregulation of these genes in galls. We also analyzed the sugar composition of the cell wall, which was drastically changed upon gall formation. In particular, the reduction of xylose suggested the reduction in the levels of xylan, which is a main component of the secondary-cell-wall-associated hemicellulose. Furthermore, the sugar composition of galls was similar to that of phytohormone-induced calluses. These results suggest that galls are composed of cells whose characteristics are related to that of callus and that phytoparasitic nematodes modulate the developmental mechanisms of the host to modify various aspects of plant physiological processes and establish a feeding site.

Materials and methods

Plant materials, nematode infection assay and preparation of gall samples

The Columbia (Col-0) accession was used as the wild-type plant of Arabidopsis. *Meloidogyne incognita* (Kofoid and White) juveniles were prepared as described previously (Nishiyama et al. 2015). Arabidopsis seeds were surface sterilized and germinated on quarter-strength MS media (Murashige and Skoog Basal Medium, Sigma) containing 0.5% sucrose (Fujifilm Wako Pure Chemical) and 0.6% (w/v) Phytagel (Sigma P8169) at pH 6.4, in 9 × 9 cm square petri dishes under continuous light at 23 °C. After the inoculation of 80 J2 nematodes in Arabidopsis seedlings at 5 days after germination, the seedlings were incubated under short-day conditions (8 h light/ 16 h dark) at 25 °C.

Self-organizing map (SOM)-based clustering of genes expressed in the root-knots

We performed a gene expression clustering analysis with the previous RNAseq data (PRJDB5797). To define differentially expressed genes (DEGs), we analyzed the mapped data by HTseq and performed ANOVA-like test (FDR < 0.01) by edgeR program, which resulted in 4,444 genes being defined

as DEGs (Robinson et al. 2010). Scaled expression values were used for multilevel 3 × 3 rectangular SOM clusters (Kohonen 1982; Wehrens and Buydens 2007). One hundred training interactions were used during clustering, and gene clusters were based on the final assignment of genes to winning units.

Analyses of the expression levels of genes that are co-expressed with cellulose-synthase-encoding genes

Genes that are co-expressed with *CESA4*, *CESA7*, and *CESA8* and with *CESA1*, *CESA3*, and *CESA6* were obtained from Persson et al. (Persson et al. 2005). The expression levels of genes were analyzed as described previously (Yamaguchi et al. 2017), the reads per kilobase per million mapped reads (RPKMs) values were calculated using Bowtie (Langmead et al. 2009) and Cuffdiff2 (ver. 2.1.1) (Trapnell et al. 2013) algorithms using the reference genome sequences (fasta) with annotation information (gff) for *A. thaliana* downloaded from the FTP sites of Ensembl Plant [https://plants.ensembl.org/index.html; Release 22]. The heatmap showing their expression levels was drawn using the heatmap2 algorithm. The analysis of xylem-related genes and *CESA* genes (Fig. S1) was performed as follows. The SR short reads obtained were divided into each sample using a demultiplexing program supplied by Illumina and were then mapped to the references described below using TopHat2 (ver. 2.0.13) (Kim et al. 2013), to calculate RPKMs for each gene using Cuffdiff2 (ver. 2.1.1) (Trapnell et al. 2013).

RT-qPCR analyses of genes that participate in the biosynthesis of the secondary cell wall

Plant tissues of 7 days post-inoculation (dpi) galls or non-inoculated roots (NIs) were immediately frozen in liquid nitrogen and homogenized with Zirconia balls (AS ONE Inc.) using a Shake Master version NEO (Biomedical Science, Inc.). Total RNA was extracted from plants using the RNeasy plant mini kit (QIAGEN Inc.), and cDNA was prepared using the Super Script III First Strand Synthesis Kit (Thermo Fisher Scientific, Inc.). The RT-qPCR analysis was conducted using StepOnePlus™ (Thermo Fisher Scientific, Inc.) with PowerUp SYBR Green Master Mix (Thermo Fisher Scientific. Inc.), according to the manufacturer's instructions. The primers used in this analysis are listed in Table S1.

High-performance anion-exchange chromatography (HPAEC)

The cell wall samples were prepared according to the procedure described by Nishitani and Masuda (1979), with minor modifications. The roots, galls, and calluses derived from the host plant were sampled and heated in 6 ml of 80% ethanol for 5 min, washed with 3 ml of 80% ethanol, then replaced two times with 5 ml of 100% ethanol for 20 min each. After the ethanol was washed out, the samples were washed with 3 ml of methanol/chloroform (1/1; v/v) twice for 10 min each, to remove lipids. The samples were then washed further with 3 ml of 100% EtOH three times, followed by three washes with 3 ml of acetone for 10 min each. After removing the acetone, the samples were dried. Trifluoroacetic acid (TFA; 500 µl, 2 N) was added to the dried sample and heated at 120 °C for 60 min, to hydrolyze non-cellulosic polysaccharides, followed by evaporation in vacuo at 45 °C. Dried hydrolysates were then suspended in 500 µl of water and centrifuged for 5 min, to obtain the supernatant, which contained monosaccharides and were then subjected to high-performance anion-exchange chromatography with pulsed amperometric detection (HPAEC-PAD) using a Dionex ICS-5000 system equipped with a CarboPac PA1 column (Dionex). The column was eluted at a flow rate of 1.1 ml min^{-1} with (1) water from 0 to 19 min, (2) followed by a linear gradient of 0 to 100 mM NaOH in water from 19 to 22 min, (3) an isocratic solution of 100 mM NaOH in water from 22 to 33 min, (4) an isocratic solution of 150 mM sodium acetate/100 mM NaOH in water from 33 to 39 min. Myo-inositol (4 µg) was used as an internal standard for the quantification of individual monosaccharides.

Gall induction and callus induction for polysaccharide analyses

Modified nematode infection medium and modified callus induction medium containing phytohormones were developed based on the callus induction medium described in Ozawa et al. (1998). Arabidopsis seeds were germinated and grown on the Modified nematode infection medium composed of Gamborg B5 salt mixture (Fujifilm Wako Pure Chemical), 2% sucrose (Fujifilm Wako Pure Chemical), 0.05% (w/v) 2-(4-morpholino) ethanesulfonic acid (MES), and 0.6% (w/v) Phytagel (Sigma P8169) at pH 5.7, in 9 × 9 cm square petri dishes under continuous light at 23 °C. After the inoculation of J2 nematodes in Arabidopsis seedlings 5 days after germination, the seedlings were incubated under short-day conditions (8 h light/16 h dark) at 25 °C.

For callus induction, 0.5 mg l^{-1} 2,4-dichlorophenoxyacetic acid (Fujifilm Wako Pure Chemical) and 0.1 mg l^{-1} kinetin (Fujifilm Wako Pure Chemical) were supplied to the modified nematode infection medium. Root explants obtained from 5 days after germination or uncut seedlings were placed on the modified callus induction medium and incubated under short-day conditions (8 h light/16 h dark) at 25 °C.

K-means clustering and principal component analysis of neutral sugar composition

The statistical analysis of neutral sugar composition was performed using the R software (R Core Team 2016). The obtained HPAEC data were studied using a hierarchical clustering and a k-means clustering analysis, for classification into two groups. The results of k-means clustering are depicted as two-dimensional plots according to PCA and an additional layer was added for the k-means clustering.

Results

Genes related to the secondary cell wall were downregulated in galls

Previously, we showed that the procambium-development-related gene regulatory network is activated during gall formation (Yamaguchi et al. 2017). In particular, a master regulatory transcription factor, MONOPTEROS (MP)/AUXIN RESPONSE FACTOR 5 (ARF5), is induced and plays a crucial role in irregular organogenesis (Barcala et al. 2010; Yamaguchi et al. 2017). Although the key molecular and physiological processes have been identified, its downstream consequences have not been deciphered. To understand further the phenomenon of gall formation, we further characterized the time-course transcriptome data for gall formation (PRJDB5797). First, we selected 4,444 DEGs detected in the transcriptome analyses by ANOVA (FDR < 0.01). Next, we classified the DEGs via SOM-based clustering, and obtained nine clusters (Fig. 1). Among them, cluster 2 represented the largest population (< 1400 genes) and most genes in this cluster were likely to be decreased upon the progression of gall formation. In our previous study, we selected six genes (i.e., *VND6*, *VND7*, *XCP1*, *XCP2*, *TED6*, and *TED7*) (Endo et al. 2009; Funk et al. 2002; Kubo et al. 2005) as xylem-related genes. In particular, four out of these six genes were decreased upon gall formation and were included in cluster 2; in contrast, neither *VND6* nor *VND7* were included in DEGs (Fig. S1). These results suggest that the secondary wall thickening and programmed cell death that take place during xylem formation are, at least in part, suppressed in the galls. Accordingly, we found that *CESA4*, *CESA7*, and *CESA8*, which encode cellulose synthases that participate in the formation of the secondary cell wall, were decreased upon the progression of gall formation (Fig. S1) and were included in cluster 2, suggesting that the population of cells that synthesize secondary cell walls is reduced in the galls.

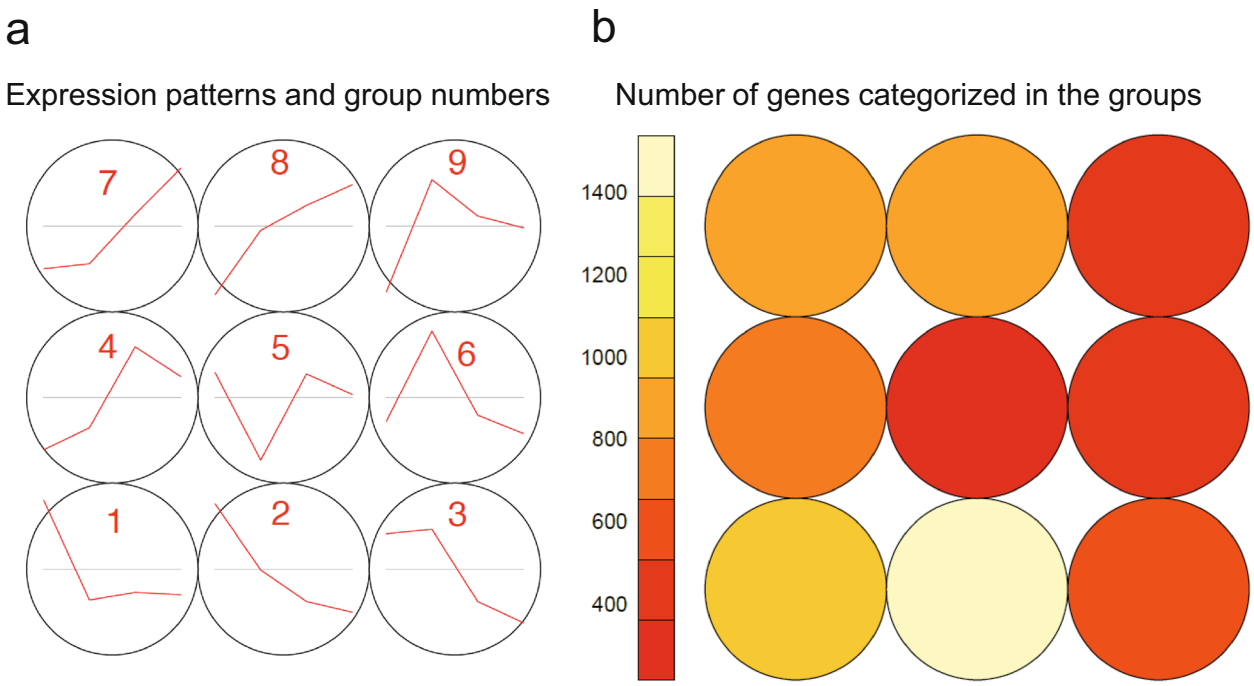

Fig. 1 SOM clustering analysis of the expression of differentially expressed genes (DEGs) and their expression profiles. **a** Results of SOM clustering. The line plots indicate representative expression patterns at NI (0 dpi), 3 dpi, 5 dpi, and 7 dpi in each cluster. For SOM and diagrams, the 3 × 3 rectangular topology is shown. **b** Number of genes assigned to each SOM cluster. The red and white colors indicate low and high counts, respectively

Genes that are co-expressed with *CESA4*, *CESA7*, and *CESA8* were decreased in galls

To assess whether the genes related to the secondary cell wall are enriched in cluster 2, we analyzed the expression profiles of cell-wall-related genes for either the primary cell wall or the secondary cell wall. Genes related to the formation of the primary cell wall were obtained from the results of co-expression analyses of genes that exhibited an expression pattern resembling *CESA1*, *CESA3*, and *CESA6*; whereas those related to the secondary cell wall were acquired from the list of genes that had an expression pattern correlating with that of *CESA4*, *CESA7*, and *CESA8* (Persson et al. 2005). As expected, most secondary-cell-wall-related genes tended to be gradually decreased during gall formation (Fig. 2a). We found 33 such DEGs among the 40 genes that were co-expressed with *CESA4*, *CESA7*, and *CESA8*; in particular, 27 out of these 33 genes were included in cluster 2 of our SOM-based clustering analysis (Table 1). In contrast, primary-cell-wall-related genes did not display an obvious trend (Fig. 2b, Table 1). The decreased levels of secondary-cell-wall-related genes were validated by quantitative RT-PCR analysis. The evaluation of the expression levels of *CESA4*, *CESA7*, *CESA8*, *IRX8*, and *IRX12* in the galls revealed that the relative amount of the mRNAs of all the selected genes was significantly reduced in galls (Fig. 2c) (Brown et al. 2005; Persson et al. 2007). These results support the notion that the secondary-cell-wall-related genes are decreased in the galls.

Neutral sugar analyses of cell wall polysaccharides support secondary cell wall formation is suppressed in gall cells

Our transcriptome analyses showed that the secondary-cell-wall-related genes were decreased in response to the formation of galls. Therefore, we decided to investigate whether the composition of the cell wall is altered in the galls. Cell walls are mainly composed of polysaccharides; hence, the monomerized sugars obtained from the tissues are thought to reflect the features of the cell wall. We performed neutral sugar analyses using high-performance anion-exchange chromatography (HPAEC), to evaluate the levels of polysaccharides. As shown in Fig. 3 and Table S2, arabinose and galactose represented 50–60% of the monosaccharides purified from both non-treated roots and galls. Galactose was slightly increased in response to the gall formation whereas arabinose and rhamnose did not show obvious changes; therefore, rhamnogalacturonan I, which is composed of the three types of sugars, was not affected in the galls. In contrast, the levels of xylose in the galls were decreased to less than 50% of that of non-inoculated root cells (Fig. 3, Table S2). Xylose is one of the main components of hemicelluloses, i.e., xylan and xyloglucan. Xylan is a polymer of xylose whereas xyloglucan is composed of a glucose backbone with a xylose sidechain. Since our neutral sugar analysis detected the increase of glucose (Fig. 3, Table S2), the decrease in the level of xylose is likely to have been caused by the reduction of xylan in the cell wall of gall cells (Zhong et al. 2019; Zhong and Ye 2014). Xylan bridges cellulose microfibrils with lignin, to reinforce the structure of the secondary cell wall (Kang et al. 2019). Collectively, our observations suggest that the secondary cell wall is decreased in gall cells.

The cell wall composition of gall cells resembles that of calluses

Previously, we showed that gall cells express genes that are associated with procambium cells, because the galls were composed of procambium-like undifferentiated cells (Yamaguchi et al. 2017). In addition, RKN is capable of inducing callus-like structure in infected leaves (Olmo et al. 2017). These observations suggested that gall formation likely accompanies induction of pluripotent cell mass and a drastic change in cellular identity leads to the rearrangement of cell wall composition. To assess whether cell wall changes rely on the induction of proliferating cells, we analyzed the cell wall composition of phytohormone-induced calluses as a representative cell population that contain, at least partially, multipotent stem cells, and compared the results with those obtained for galls. Callus induction, in principle, was achieved by the treatment of precise phytohormones and the requirements of media condition is not strict. For this assay, we developed a modified callus-induction medium by adding phytohormones to the RKN infection medium. We confirmed the efficient induction of calluses from seedlings and root explants in this condition (Fig. S2). These calluses were subjected to HPAEC analysis. Our triplicate measurements suggested that the content of galactose tended to be increased and that of xylose tended to be decreased in cell walls purified from callus cells (Fig. 4a, Table S3).

Statistical analyses emphasize the similarities between gall and callus cells

We performed a hierarchical clustering analysis of the results of the neutral sugar composition experiment. The values of cell wall composition obtained for galls resembled those of calluses derived from seedlings. Simultaneously, the values of cell wall composition obtained from root explant derived calluses are grouped with them whereas non-treated roots were classified into the outgroup. This finding suggests that the cell wall composition of galls is relatively similar to that of calluses, rather than to that of non-treated roots

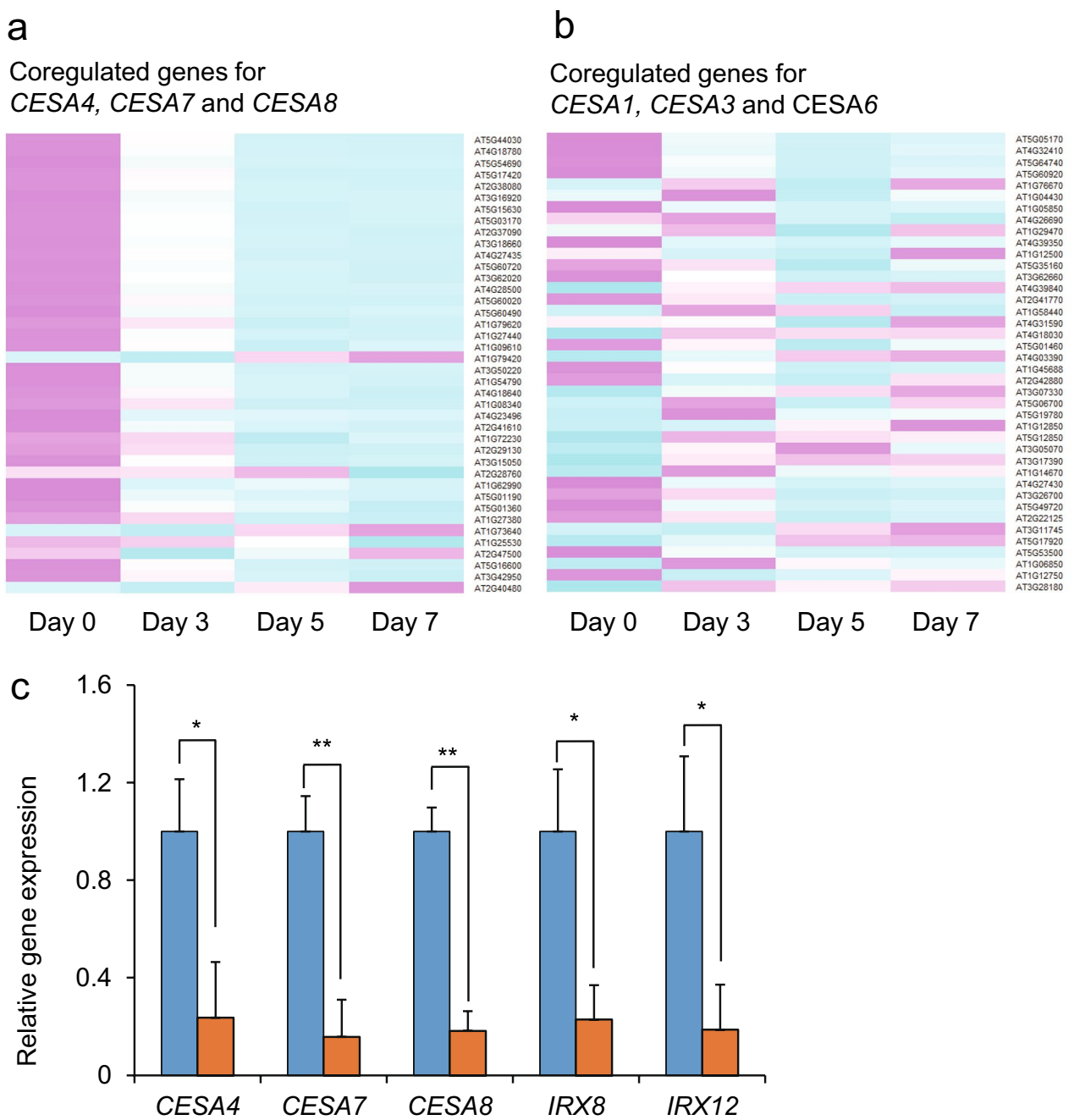

Fig. 2 Secondary-cell-wall-related genes were decreased in galls. Comparison of genes that were co-expressed with cellulose synthases: **a** *CESA1*, *CESA3*, and *CESA6* and **b** *CESA4*, *CESA7*, and *CESA8*. The magenta color indicates genes that were upregulated compared with the median levels of the four samples, and the cyan color denotes the decrease in the amount of mRNAs in the heat map. The list of co-expressed genes was obtained from Persson et al. (2005). **c** Decreased levels of secondary-cell-wall-related genes in root-knot 7 days after inoculation. Quantitative RT–PCR was performed using total RNA extracted from root-knot 7 days after inoculation and from the wild-type root, as an uninfected control. The expression level of each gene was divided by the expression level of the PP2AA3 (*AT1G13320*) gene; the normalized expression level in the control was set to 1. The error bars indicate the SD of three biological replicates. The single and double asterisks represent $P < 0.05$ and $P < 0.01$, respectively, as calculated using Welch's *t* test

Table 1 SOM-based clustering of genes that are co-expressed with CESAs

	CESA4/7/8	CESA1/3/6
Group 1	2	4
Group 2	27	6
Group 3	1	0
Group 4	0	0
Group 5	0	0
Group 6	0	1
Group 7	3	2
Group 8	0	4
Group 9	0	1
Total	33	18
Non DEG	7	22

(Fig. 4b). Furthermore, k-means clustering into two groups also revealed that the neutral sugar ratio of galls resembles that of calluses (Fig. 4c). These results are consistent with the notion that the composition of the cell walls of galls resembles that of callus cells.

Discussion

Higher organisms, including seed plants, have evolved sophisticated developmental regulation mechanisms. In the steady state, they routinely develop leaves, flowers, or roots based on the genetically encoded body plan. However, biotic and abiotic stimuli often impair this program and sometimes induce organ malformation. Such irregular organogenesis, including the acquisition of atypical characteristics of cells stimulated by parasitism, is an interesting event in nature. The formation of galls induced by plant parasitic RKNs is representative of irregular organogenesis (Bartlem et al. 2014; Escobar et al. 2015; Gheysen and Mitchum 2009). Previous studies reported that various morphological alterations accompany gall formation, e.g., GC/NC induction and rearrangement of the vasculature in the parasitized roots (Bartlem et al. 2014; Bird 1961; de Almeida Engler and Gheysen 2013; Jones and Goto 2011). The present study revealed that a drastic rearrangement in cell wall composition occurred upon gall formation.

The transcriptome analyses showed that cell-wall-related genes were changed in response to gall formation. Specifically, secondary-cell-wall-associated genes, including CESA4, CESA7, CESA8 and their co-expressed genes, appeared to be decreased. Consistent with the gene expression analysis, the assessment of the cell wall composition implied that the amount of xylose enriched in the secondary cell wall is reduced in the galls. Although the global transcriptome provides a plausible explanation for the changes in cell wall composition, the specific genes that are responsible for the changes need to be identified. Moreover, we developed a callus-induction system by modifying the nematode infection assay medium and performing an HPAEC analysis, to determine the composition of the cell walls of undifferentiated cell populations. The neutral sugar analyses, in combination with statistical analyses, revealed that the cell wall composition of galls resembles that of calluses. Callus is a mass of

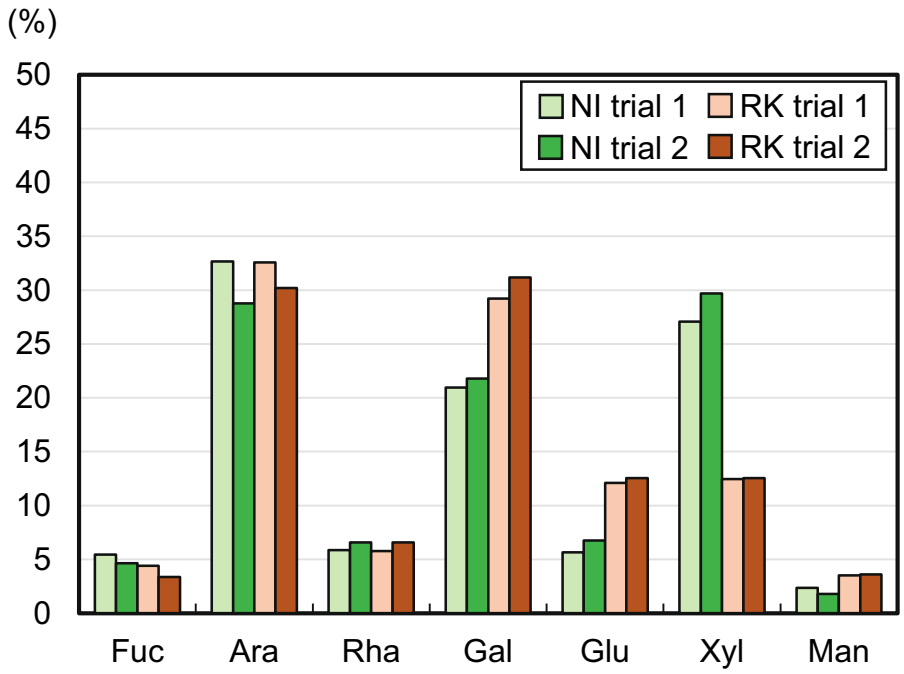

Fig. 3 HPAEC analyses of neutral sugars obtained from root-knots or non-infected root cells at 14 dpi root-knots grown on MS-based infection medium. The complete data pertaining to the monosaccharide ratio are shown in Table S2. *Fuc* fucose, *Ara* arabinose, *Rha* rhamnose, *Gal* galactose, *Glu* glucose, *Xyl* xylose, *Man* mannose

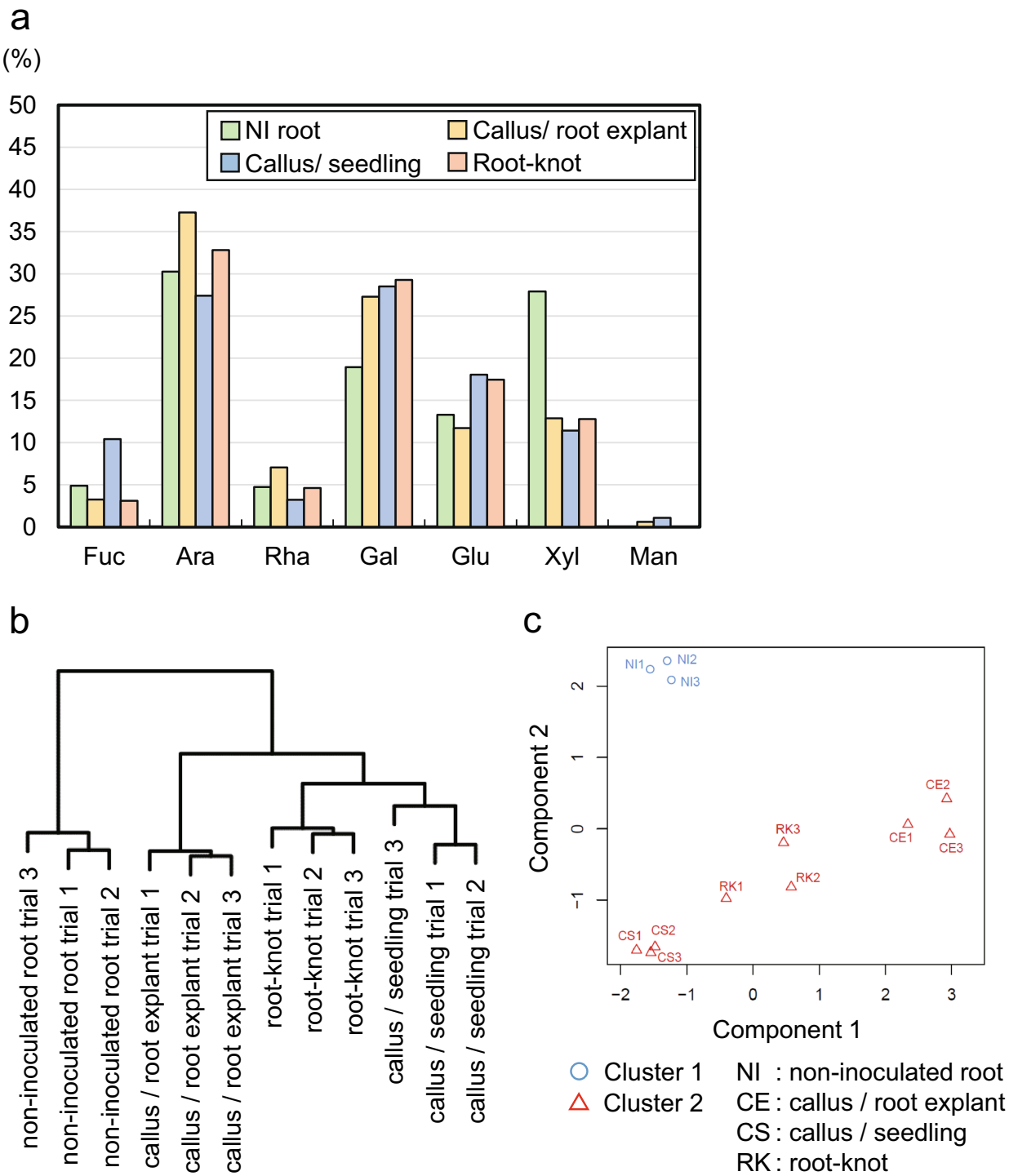

Fig. 4 The cell wall composition of root-knot cells resembled that of undifferentiated cells. **a** HPAEC analyses of neutral sugars obtained from 14 dpi root-knots, non-infected root cells, and 14 day after induction calluses prepared from root explants and seedlings grown on B5-based medium. Result of first measurement was shown, while similar trends were obtained in additional two replicates. The complete data obtained for the monosaccharide ratio are shown in Table S3. *Fuc* fucose, *Ara* arabinose, *Rha* rhamnose, *Gal* galactose, *Glu* glucose, *Xyl* xylose, *Man* mannose. **b** Hierarchical clustering of the neutral sugar composition of gall cells and callus cells. Comparison of neutral sugar composition with root-explant-derived or seedling-derived-calluses. **c** The results of *k* means clustering analyses were evaluated by a principal component analysis (PCA) of the percentage of sugar values from the crude cell wall material. The first two components explained 74.1% of the variation

proliferating cells that derived from various types of tissue and are known to contain, at least partially, cells that have the ability to regenerate (Sugimoto et al. 2011). Thus, the resemblance of gall cells to the callus, together with that to procambial cells shown in our previous study, support the notion that a gall is composed of a significant amount of cells that share the characteristics of stem cells.

Disrupting the cell wall of host plants would be an important step in the infection, as nematodes can secret degrading enzymes (Davis et al. 2011; Wieczorek 2015). This may affect the cell wall content in the host root; however, the extent of the cell wall degradation by nematode-derived enzymes is thought to be limited around the nematode. Therefore, the observed alteration in cell wall composition is likely to depend on the cell identity included in the galls.

One of the characteristic features of gall formation is GC/NC induction at the feeding site of the nematodes. GCs are generated through atypical cell cycle events, including acytokinetic mitosis, which induces multinucleation in a cell and genome-multiplicating endoreduplication cycle (de Almeida Engler et al. 2011; de Almeida Engler and Gheysen 2013). In addition, NCs are actively proliferating structures that cause organ knotting in the roots. Because both GCs and NCs require an active cell cycle, these cells share some features with undifferentiated stem cells. Accordingly, our previous study showed that procambium-associated genes are induced in the galls (Yamaguchi et al. 2017). These findings led us to propose an attractive hypothesis: once the nematodes invade the host vasculature, they stimulate procambial cells to modulate their cellular machinery to become NCs or GCs. Although a carefully designed cell lineage tracing is needed to depict the developmental trajectory of the gall cells, analyses focusing on cellular identity will provide insights into the induction of the atypical cells and accompanying cell wall modifications. Taken together, our findings provide additional insights regarding gall cells and will help establish a global scenario of parasite-induced atypical organ formation processes.

Acknowledgements We thank Ms. Tomomi Sagara (Kumamoto University) for technical assistance.

Author contributions TI and SS initiated the project and designed the experiments. RS perform infection assays. TI, SN and SK performed statistical analyses. RS, SS, MTN and NM performed expression analyses. TK, RY and KN performed neutral sugar measurements. SS advised on the planning of the project and writing. TI wrote the manuscript with input from all authors.

Funding This work was supported by grants from the Japan Society for the Promotion of Science (JSPS) KAKENHI [Grant numbers 26440151, 14J40052, 25440134, 25119713, 24114009, 24370024, 16K14757, 17H03967, and 18H05487 to S.S., 18H04787 and 18H04844 to S.K.], by the MEXT Supported Program for the Strategic Research Foundation at Private Universities from the Ministry of Education, Culture, Sports, Science and Technology of Japan, Grant Number S1511023 to S. K. and partly supported by ALCA program of the Japan Science and Technology Agency (Grant no. JPMJAL1107).

Compliance with ethical standards

Conflict of interest The authors declare no conflicts of interest associated with this research or manuscript.

References

Arioli T, Peng L, Betzner AS, Burn J, Wittke W, Herth W, Camilleri C, Hofte H, Plazinski J, Birch R, Cork A, Glover J, Redmond J, Williamson RE (1998) Molecular analysis of cellulose biosynthesis in Arabidopsis. Science 279:717–720

Barcala M, Garcia A, Cabrera J, Casson S, Lindsey K, Favery B, Garcia-Casado G, Solano R, Fenoll C, Escobar C (2010) Early transcriptomic events in microdissected Arabidopsis nematode-induced giant cells. Plant J 61:698–712

Bartlem DG, Jones MG, Hammes UZ (2014) Vascularization and nutrient delivery at root-knot nematode feeding sites in host roots. J Exp Bot 65:1789–1798

Bird AF (1961) The ultrastructure and histochemistry of a nematode-induced giant cell. J Biophys Biochem Cytol 11:701–715

Brown DM, Zeef LA, Ellis J, Goodacre R, Turner SR (2005) Identification of novel genes in Arabidopsis involved in secondary cell wall formation using expression profiling and reverse genetics. Plant Cell 17:2281–2295

Cabrera J, Diaz-Manzano FE, Barcala M, Arganda-Carreras I, de Almeida-Engler J, Engler G, Fenoll C, Escobar C (2015) Phenotyping nematode feeding sites: three-dimensional reconstruction and volumetric measurements of giant cells induced by root-knot nematodes in Arabidopsis. New Phytol 206:868–880

Davis EL, Haegeman A, Kikuchi T (2011) Degradation of the plant cell wall by nematodes. In: Jones J, Gheysen G, Fenoll C (eds) Genomics and molecular genetics of plant–nematode interactions. Springer Netherlands, Dordrecht, pp 255–272

de Almeida EJ, Engler G, Gheysen G (2011) Unravelling the plant cell cycle in nematode induced feeding sites. In: Jones J, Gheysen G, Fenoll C (eds) Genomics and molecular genetics of plant–nematode interactions. Springer Netherlands, Dordrecht, pp 349–368

de Almeida EJ, Gheysen G (2013) Nematode-induced endoreduplication in plant host cells: why and how? Mol Plant Microbe Interact 26:17–24

Endo S, Pesquet E, Yamaguchi M, Tashiro G, Sato M, Toyooka K, Nishikubo N, Udagawa-Motose M, Kubo M, Fukuda H, Demura T (2009) Identifying new components participating in the secondary cell wall formation of vessel elements in zinnia and Arabidopsis. Plant Cell 21:1155–1165

Escobar C, Barcala M, Cabrera J, Fenoll C (2015) Chapter one—overview of root-knot nematodes and giant cells. In: Carolina E, Carmen F (eds) Advances in botanical research, vol 73. Academic Press, Cambridge, pp 1–32

Fagard M, Desnos T, Desprez T, Goubet F, Refregier G, Mouille G, McCann M, Rayon C, Vernhettes S, Hofte H (2000) PROCUSTE1 encodes a cellulose synthase required for normal cell elongation specifically in roots and dark-grown hypocotyls of Arabidopsis. Plant Cell 12:2409–2424

Funk V, Kositsup B, Zhao C, Beers EP (2002) The Arabidopsis xylem peptidase XCP1 is a tracheary element vacuolar protein that may be a papain ortholog. Plant Physiol 128:84–94

Gheysen G, Mitchum MG (2009) Molecular insights in the susceptible plant response to nematode infection. In: Berg RH, Taylor

CG (eds) Cell biology of plant nematode parasitism. Springer, Berlin, pp 45–81
Jones MGK, Goto DB (2011) Root-knot nematodes and giant cells. In: Jones J, Gheysen G, Fenoll C (eds) Genomics and molecular genetics of plant-nematode interactions. Springer Netherlands, Dordrecht, pp 83–100
Kang X, Kirui A, Dickwella Widanage MC, Mentink-Vigier F, Cosgrove DJ, Wang T (2019) Lignin–polysaccharide interactions in plant secondary cell walls revealed by solid-state NMR. Nat Commun 10:347
Kim D, Pertea G, Trapnell C, Pimentel H, Kelley R, Salzberg SL (2013) TopHat2: accurate alignment of transcriptomes in the presence of insertions, deletions and gene fusions. Genome Biol 14:R36
Kohonen T (1982) Self-organized formation of topologically correct feature maps. Biol Cybern 43:59–69
Kubo M, Udagawa M, Nishikubo N, Horiguchi G, Yamaguchi M, Ito J, Mimura T, Fukuda H, Demura T (2005) Transcription switches for protoxylem and metaxylem vessel formation. Genes Dev 19:1855–1860
Langmead B, Trapnell C, Pop M, Salzberg SL (2009) Ultrafast and memory-efficient alignment of short DNA sequences to the human genome. Genome Biol 10:R25
Li S, Bashline L, Lei L, Gu Y (2014) Cellulose synthesis and its regulation. Arabidopsis Book 12:e0169
Nishitani K, Masuda Y (1979) Growth and cell wall changes in azuki bean epicotyls I. Changes in wall polysaccharides during intact growth. Plant Cell Physiol 20:63–74
Nishiyama H, Ngan BT, Nakagami S, Ejima C, Ishida T, Sawa S (2015) Protocol for root-knot nematode culture by a hydroponic system and nematode inoculation to Arabidopsis. Nematol Res (Jpn J Nematol) 45:45–49
Olmo R, Cabrera J, Moreno-Risueno MA, Fukaki H, Fenoll C, Escobar C (2017) Molecular transducers from roots are triggered in Arabidopsis leaves by root-knot nematodes for successful feeding site formation: a conserved post-embryogenic de novo organogenesis program? Front Plant Sci 8:875
Ozawa S, Yasutani I, Fukuda H, Komamine A, Sugiyama M (1998) Organogenic responses in tissue culture of SRD mutants of *Arabidopsis thaliana*. Development 125:135–142
Persson S, Caffall KH, Freshour G, Hilley MT, Bauer S, Poindexter P, Hahn MG, Mohnen D, Somerville C (2007) The Arabidopsis irregular xylem8 mutant is deficient in glucuronoxylan and homogalacturonan, which are essential for secondary cell wall integrity. Plant Cell 19:237–255
Persson S, Wei H, Milne J, Page GP, Somerville CR (2005) Identification of genes required for cellulose synthesis by regression analysis of public microarray data sets. Proc Nat Acad Sci USA 102:8633–8638
R Core Team (2016) R: a language and environment for statistical computing. R Foundation for Statistical Computing
Robinson MD, McCarthy DJ, Smyth GK (2010) edgeR: a Bioconductor package for differential expression analysis of digital gene expression data. Bioinformatics 26:139–140
Scheible WR, Eshed R, Richmond T, Delmer D, Somerville C (2001) Modifications of cellulose synthase confer resistance to isoxaben and thiazolidinone herbicides in Arabidopsis Ixr1 mutants. Proc Nat Acad Sci USA 98:10079–10084
Sugimoto K, Gordon SP, Meyerowitz EM (2011) Regeneration in plants and animals: dedifferentiation, transdifferentiation, or just differentiation? Trends Cell Biol 21:212–218
Taylor NG, Howells RM, Huttly AK, Vickers K, Turner SR (2003) Interactions among three distinct CesA proteins essential for cellulose synthesis. Proc Nat Acad Sci USA 100:1450–1455
Taylor NG, Laurie S, Turner SR (2000) Multiple cellulose synthase catalytic subunits are required for cellulose synthesis in Arabidopsis. Plant Cell 12:2529–2540
Taylor NG, Scheible WR, Cutler S, Somerville CR, Turner SR (1999) The irregular xylem3 locus of Arabidopsis encodes a cellulose synthase required for secondary cell wall synthesis. Plant Cell 11:769–780
Trapnell C, Hendrickson DG, Sauvageau M, Goff L, Rinn JL, Pachter L (2013) Differential analysis of gene regulation at transcript resolution with RNA-seq. Nat Biotechnol 31:46–53
Wehrens R, Buydens LMC (2007) Self- and super-organizing maps in R: The Kohonen Package. J Stat Soft 21:1
Wieczorek K (2015) Chapter three—cell wall alterations in nematode-infected roots. In: Escobar C, Fenoll C (eds) Advances in botanical research, vol 73. Academic Press, Cambridge, pp 61–90
Yamaguchi YL, Suzuki R, Cabrera J, Nakagami S, Sagara T, Ejima C, Sano R, Aoki Y, Olmo R, Kurata T, Obayashi T, Demura T, Ishida T, Escobar C, Sawa S (2017) Root-knot and cyst nematodes activate Procambium-associated genes in Arabidopsis roots. Front Plant Sci 8:1195
Zhong R, Cui D, Ye ZH (2019) Secondary cell wall biosynthesis. New Phytol 221:1703–1723
Zhong R, Ye Z-H (2014) Secondary cell walls: biosynthesis, patterned deposition and transcriptional regulation. Plant Cell Physiol 56:195–214